



HAL
open science

Contact Mechanics Of Microscopically Rough Surfaces With Graded Elasticity

Marco Paggi, Giorgio Zavarise

► **To cite this version:**

Marco Paggi, Giorgio Zavarise. Contact Mechanics Of Microscopically Rough Surfaces With Graded Elasticity. European Journal of Mechanics - A/Solids, 2011, 30 (5), pp.696. 10.1016/j.euromechsol.2011.04.007 . hal-00769686

HAL Id: hal-00769686

<https://hal.science/hal-00769686>

Submitted on 3 Jan 2013

HAL is a multi-disciplinary open access archive for the deposit and dissemination of scientific research documents, whether they are published or not. The documents may come from teaching and research institutions in France or abroad, or from public or private research centers.

L'archive ouverte pluridisciplinaire **HAL**, est destinée au dépôt et à la diffusion de documents scientifiques de niveau recherche, publiés ou non, émanant des établissements d'enseignement et de recherche français ou étrangers, des laboratoires publics ou privés.

Accepted Manuscript

Title: Contact Mechanics Of Microscopically Rough Surfaces With Graded Elasticity

Authors: Marco Paggi, Giorgio Zavarise

PII: S0997-7538(11)00053-2

DOI: [10.1016/j.euromechsol.2011.04.007](https://doi.org/10.1016/j.euromechsol.2011.04.007)

Reference: EJMSOL 2705

To appear in: *European Journal of Mechanics / A Solids*

Received Date: 6 January 2011

Revised Date: 6 April 2011

Accepted Date: 18 April 2011

Please cite this article as: Paggi, M., Zavarise, G. Contact Mechanics Of Microscopically Rough Surfaces With Graded Elasticity, *European Journal of Mechanics / A Solids* (2011), doi: 10.1016/j.euromechsol.2011.04.007

This is a PDF file of an unedited manuscript that has been accepted for publication. As a service to our customers we are providing this early version of the manuscript. The manuscript will undergo copyediting, typesetting, and review of the resulting proof before it is published in its final form. Please note that during the production process errors may be discovered which could affect the content, and all legal disclaimers that apply to the journal pertain.



Contact mechanics of microscopically rough surfaces with graded elasticity

Marco Paggi¹ and Giorgio Zavarise²

¹*Leibniz Universität Hannover, Institut für Kontinuumsmechanik, Appelstraße 11
30167 Hannover, Germany. On leave from Department of Structural and Geotechnical Engineering,
Politecnico di Torino, Torino, Italy
paggi@ikm.uni-hannover.de, marco.paggi@polito.it*

²*Department of Innovation Engineering, University of Salento, Italy
giorgio.zavarise@unisalento.it*

Abstract. The well-known Greenwood and Williamson contact theory for microscopically homogeneous rough surfaces is generalized by considering functionally graded elastic rough surfaces. In particular, two distinct cases giving rise to a non-constant Young's modulus with depth are considered: (I) an initially plane layered (or graded) solid which is non-uniformly eroded so that the final product is a rough surface with asperities having an elastic modulus depending on the height; and (II) an initially homogeneous rough surface which receives a surface treatment or a chemical degradation which modify the elastic properties of the asperities as a function of the depth from the exposed surface. These Functionally Graded Surfaces (FGS) can be observed both in biological systems and in mechanical components. The effects of graded elasticity on the relationship between real contact area and applied load and on the plasticity index are quantified and illustrated with numerical examples. It will be shown that the contact response may differ up to one order of magnitude with respect to that of a homogeneous surface. Comparison between Case I and Case II also shows that, for special surface properties, the two types of grading can provide the same mechanical response.

Keywords: Contact mechanics, rough surfaces, functionally graded surfaces, graded elasticity, finite elements.

1. Introduction

Tribological contacts often involve surfaces covered by films of other materials. The bulk material presents also a different structure of the grains, which results into a deep

variation of the mechanical characteristics (Rabinowicz, 1995). A typical example is shown in Fig. 1, where the formation of thin layers due to chemical interactions with the environment, and the dependence of the grain size on the depth due to material processing are evidenced. These films may be adventitious (for example, due to chemical reaction with the environment), they may arise as a result of the rubbing process, or they may be deliberately formed using special techniques, like carburizing or nitriding processes. Clearly, as the film thickness tends to zero, the behaviour is determined entirely by the properties of the substrate. On the contrary, when the film thickness becomes sufficiently large, the behaviour is determined entirely by the properties of the film. Between these two extremes, the behaviour is a function of the properties both of the film and of the substrate materials. Classical examples are the variation of microhardness and contact conductance for lead films of various thicknesses on mild steel substrates (Hegazy, 1985; Yovanovich, 2005). More importantly, the wear resistance of any surface is dependent on both the hardness and the elastic modulus of the contacting surface. Hence, a relatively thin surface film can modify both these tribological properties.

[Figure 1 about here]

A similar grading takes place in many biological systems, where natural selection has optimized the surface properties for achieving an optimal functionality. Thus, for example, the adhesion pads on many insects consist of graded materials which may exhibit robust flow tolerant adhesion (Sherge and Gorb, 2001; Gao et al., 2004). In this case, the elastic grading is the result of a cellular microstructure with a nonuniform cell size, e.g. see Fig. 2, where the dependence of the cell size on the depth from the surface is shown. These situations can be mimicked by performing a non-uniform erosion of an initially layered or graded solid.

[Figure 2 about here]

The microscopical contact theory by Greenwood and Williamson (1966) can be used to characterize the contact behaviour of homogeneous rough surfaces taking into

account their stochastic properties. To simplify the properties of rough surfaces as detailed later also by Nayak (1971), Greenwood and Williamson (1966) assumed that the asperities have the same radius of curvature whatever their height and that the asperities are axisymmetric, so that they produce circular contact areas when loaded. Considering the contact of each asperity as governed by the Hertzian theory, they obtained the expressions of the total real contact area, A , and of the load, P , as functions of the dimensionless mean plane separation, d/σ , where σ is the surface roughness. The derived equations are quite general, since they depend on three parameters: the asperity density, the mean radius of curvature of the asperities and the standard deviation of the asperity height Gaussian distribution. This made the Greenwood and Williamson contact theory prone to be generalized and extended. So far, most of the existing improvements and generalizations have concerned the description of the geometric properties of the surface. The model by Bush et al. (1975), for instance, takes into account a distribution of asperity curvatures in the calculation, rather than using an average value. The original formulation has been recently re-examined also by Greenwood (2006) himself (see also Zavarise et al. (2004, 2007) for a models overview). McCool (1992) adopted a Weibull distribution of asperity heights and analyzed the effect of skewness and kurtosis on the predicted contact results. Another significant generalization of the original Greenwood and Williamson contact theory was proposed by Ciavarella et al. (2008) and by Paggi and Ciavarella (2010), taking into account the effect of asperity interaction which was neglected in the original formulation.

All of these variants of the original model can be applied when contact involves at most two different materials. To deal with layered systems, McCool (1990, 2000) extended the capabilities of the original Greenwood and Williamson contact theory to the problem of elastic contact of coated rough surfaces, where a homogeneous rough interface of finite thickness is considered as mounted over a homogeneous elastic medium with different elastic properties.

To our best knowledge, no comprehensive theory has been proposed so far in order to deal with the problem of contact mechanics of rough interfaces with functionally graded elastic properties. Theoretical models for contact mechanics of Functionally Graded Materials (FGM) are in fact quite recent, and only a few studies concerning smooth surfaces are available in the literature. Among them, we mention the recent paper by

Liu et al. (2008), where the indentation of a half-space made of a FGM is analyzed with reference to spherical or conical indenters or even in the case of a flat elastic punch. Giannakopoulos and Suresh (1997a, b) investigated the indentation of solids with graded elastic properties. Lee et al. (2009) considered the effect of an elastic modulus that decreases with depth on the load-displacement relation for indentation of a graded half space by a rigid indenter.

In this paper we propose a generalization of the Greenwood and Williamson contact theory to the case of Functionally Graded Surfaces (FGS). We consider two distinct cases, one represented by locally homogeneous asperities with different elastic moduli, referred to as Case I in the sequel, and another represented by locally heterogeneous asperities, referred to as Case II. In the former case, the asperities are all individually made of a homogeneous material, but the effective elastic modulus of each asperity depends on its height z above a given surface datum (see the sketch in Fig. 3(a)). This situation takes place when the elastic properties are a unique function of distance from a representative plane, as would be the case if an initially plane layered or graded solid were eroded non-uniformly so as to leave a rough surface. In the latter, the asperities are identical, but they are themselves graded. This would be appropriate if an initially rough and homogeneous surface were treated so as to modify the surface properties in a way that was a unique function of the distance from the (rough) exposed surface (see the sketch in Fig. 3(b)). Both types of FGS will be discussed in the next sections.

[Figure 3 about here]

2. Generalization of the Greenwood and Williamson contact theory to functionally graded rough surfaces

Assuming axisymmetric asperities with the same radius of curvature whatever their height, the Greenwood and Williamson (1966) theory considers the contact between a rough surface and an ideal rigid plane. The contact between two rough surfaces can be treated as the contact between an equivalent rough surface, defined by suitable composite geometrical parameters and mechanical properties, and an ideal rigid plane, see, e.g., (Zavarise et al., 2004) for a review. Considering the contact of each asperity as

governed by the Hertzian theory, the expressions of the real contact area, A , and of the load, P , as functions of the dimensionless mean plane separation, $h = d / \sigma$, is obtained in (Greenwood and Williamson, 1966) as

$$A = \pi A_n \eta \sigma \rho F_1(h) \quad (1)$$

$$P = \frac{4}{3} A_n \eta E^* \rho^{1/2} \sigma^{3/2} F_{3/2}(h) \quad (2)$$

where A_n is the nominal (or apparent) contact area, η is the surface asperity density,

$E^* = \left[(1 - \nu_1^2) / E_1 + (1 - \nu_2^2) / E_2 \right]^{-1}$ is the composite Young's modulus of the materials 1

and 2, $\rho = (1 / \rho_1 + 1 / \rho_2)^{-1}$ is the mean radius of curvature of the asperities, and

$\sigma = \sqrt{\sigma_1^2 + \sigma_2^2}$ is the r.m.s. of the distribution of asperity heights. The integrals $F_n(h)$ are given by the following expression in case of a Gaussian distribution of asperity heights

$$F_n(h) \equiv \frac{1}{\sqrt{2\pi}} \int_h^\infty (s - h)^n \exp(-0.5s^2) ds \quad (3)$$

where $s = z / \sigma$ is the dimensionless height of a generic asperity.

Starting from these results, in the next subsections we generalize the Greenwood and Williamson contact theory to the previously discussed FGM cases I and II.

2.1 Case I: Non-uniform erosion of a layered solid

Let us consider a rough surface composed of asperities with a composite Young's modulus dependent on the z coordinate, i.e., $E^*(z)$, according to a predetermined variation. Without any loss of generality, the origin of reference system can be set in correspondence of the mean plane of the asperity heights. In this type of grading, the asperities are all individually made of a homogeneous material, but the effective elastic modulus of each asperity depends on its height above the surface datum. Under these conditions, the relationship between real contact area and mean plane separation in Eq. (1) still remains valid, since it does not depend on the elastic properties of the bodies in contact. On the other hand, the relationship between load and mean plane separation in Eq. (2) is significantly affected by the presence of a non-uniform elastic modulus. In

this case, neglecting the effect of asperity interaction, as also in the original Greenwood and Williamson contact theory, and considering the expression for $F_n(h)$ in Eq. (3), the generalized Eq. (2) becomes

$$P = \frac{4}{3} A_n \eta \rho^{1/2} \sigma^{3/2} \frac{1}{\sqrt{2\pi}} \int_{d/\sigma}^{\infty} (s - d/\sigma)^{3/2} \exp(-0.5s^2) E^*(s) ds \quad (4)$$

where E^* is now included in the integral, being dependent on the variable s . Equation (4) is very general and, depending on the chosen function $E^*(s)$, different shapes of grading can be considered, i.e., linear, exponential, power-law, etc. In this treatment, the exponent 3/2 in Eq. (4) does not change, since the local behaviour of each homogeneous asperity is governed by the Hertzian law. No closed-form solutions to Eq. (4) can be found for a general grading, and a numerical integration scheme has to be pursued.

To fix ideas, and without any loss of generality, let us consider the following grading:

$$E^*(z) = \begin{cases} E^* + E'(z - z_1), & \text{for } z \leq z_1 \\ E^*, & \text{for } z \geq z_1 \end{cases} \quad (5)$$

where E' is the gradient of the Young's modulus. Equation (5) corresponds to a linearly variable Young's modulus. To introduce Eq. (5) into Eq. (4), Eq. (5) has to be written in terms of the dimensionless asperity height $s = z/\sigma$:

$$E^*(s) = \begin{cases} E^* [1 + \alpha(s - h_1)], & \text{for } s \leq h_1 \\ E^*, & \text{for } s \geq h_1 \end{cases} \quad (6)$$

where $h_1 = z_1/\sigma$ and $\alpha = \sigma E'/E^*$ is a dimensionless parameter (see Fig. 4). If $\alpha > 0$, then we have a *positive grading* and the elastic modulus is an increasing function of s moving from the mean plane towards the taller asperities in the range $s < h_1$, up to the value E^* for $s = h_1$. If $\alpha < 0$, then we have a *negative grading*, the elastic modulus is a decreasing function of s and E^* is the minimum value reached at $s = h_1$. The case $\alpha = 0$ would correspond to a homogeneous surface. Note that the physical condition $E^*(s) > 0$ imposes an upper bound to α . In particular, exploring the height range $0 < s < \infty$, we need $\alpha \leq 1/h_1$ in order to have a positive Young's modulus for all the asperities in contact.

[Figure 4 about here]

According to Eq. (6), Eq. (4) is modified as follows, depending on the final mean plane separation distance, $h = d / \sigma$, which can be either higher or lower than h_1 but usually positive valued ($h \geq 0$):

$$P^I = \begin{cases} \frac{4}{3} A_n \eta \rho^{1/2} \sigma^{3/2} \frac{E^*}{\sqrt{2\pi}} \int_h^\infty (s-h)^{3/2} \exp(-0.5s^2) ds, & \text{for } h_1 \leq h < \infty \\ \frac{4}{3} A_n \eta \rho^{1/2} \sigma^{3/2} \frac{E^*}{\sqrt{2\pi}} \left[\int_h^\infty (s-h)^{3/2} \exp(-0.5s^2) ds \right. \\ \left. + \alpha \int_h^{h_1} (s-h)^{3/2} \exp(-0.5s^2) (s-h_1) ds \right], & \text{for } h \leq h_1 \end{cases} \quad (7)$$

In the range $h_1 \leq h < \infty$, the total load is simply that of a homogeneous surface with elastic modulus E^* . In the range $h \leq h_1$, the total load is given by the sum of two contributions, one due to the asperities with elastic modulus equal to E^* , and another due to the asperities with an elastic modulus linearly depending on the height. The relative amount of these two contributions to the total load significantly depends on the variable h_1 . For instance, if $h_1 \square 3$, then we are on the tail of the Gaussian distribution of asperity heights and only few asperities would fall in that region. The probability of find an asperity taller than $h_1 = 3$ is in fact equal to 0.14%. As a consequence, the first contribution would be negligible. A parametric analysis will be performed in the next section in order to elucidate this effect.

To solve Eq. (7) numerically, we perform the change of variable $t = \exp(-s)$, obtaining $s = -\ln t$ and $ds = -dt/t$. In this way, the integration limits become finite and we get

$$P^I = \begin{cases} \frac{4}{3} A_n \eta \rho^{1/2} \sigma^{3/2} \frac{E^*}{\sqrt{2\pi}} \int_0^{\exp(-h)} (-\ln t - h)^{3/2} \exp\left(-\frac{\ln^2 t}{2}\right) \frac{1}{t} dt, & \text{for } h_1 \leq h < \infty \\ \frac{4}{3} A_n \eta \rho^{1/2} \sigma^{3/2} \frac{E^*}{\sqrt{2\pi}} \left[\int_0^{\exp(-h)} (-\ln t - h)^{3/2} \exp\left(-\frac{\ln^2 t}{2}\right) \frac{1}{t} dt \right. \\ \left. + \alpha \int_{\exp(-h_1)}^{\exp(-h)} (-\ln t - h)^{3/2} \exp\left(-\frac{\ln^2 t}{2}\right) (-\ln t - h_1) \frac{1}{t} dt \right], & \text{for } h \leq h_1 \end{cases} \quad (8)$$

Now a suitable application of the Gauss-Legendre quadrature method (Zavarise et al., 1992) (see also (Morandi Cecchi et al., 1995) for a critical examination of the accuracy of this numerical scheme when applied to the classical Greenwood and Williamson equations) gives:

$$P^I = \begin{cases} \frac{4}{3} A_n \eta \rho^{1/2} \sigma^{3/2} \frac{E^*}{\sqrt{2\pi}} \sum_{i=1}^{NGP} B_i^* (-\ln x_i^* - h)^{3/2} \exp\left(-\frac{\ln^2 x_i^*}{2}\right) \frac{1}{x_i^*}, & \text{for } h_1 \leq h < \infty \\ \frac{4}{3} A_n \eta \rho^{1/2} \sigma^{3/2} \frac{E^*}{\sqrt{2\pi}} \left[\sum_{i=1}^{NGP} B_i^* (-\ln x_i^* - h)^{3/2} \exp\left(-\frac{\ln^2 x_i^*}{2}\right) \frac{1}{x_i^*} \right. \\ \left. + \alpha \sum_{i=1}^{NGP} B_i^{**} (-\ln x_i^{**} - h)^{3/2} \exp\left(-\frac{\ln^2 x_i^{**}}{2}\right) \frac{(-\ln x_i^{**} - h_1)}{x_i^{**}} \right], & \text{for } h \leq h_1 \end{cases} \quad (9)$$

where:

$$x_i^* = \exp(-h) \frac{(1 + x_i)}{2} \quad (10a)$$

$$B_i^* = \frac{\exp(-h)}{2} B_i \quad (10b)$$

$$x_i^{**} = \frac{\exp(-h) - \exp(-h_1)}{2} x_i + \frac{\exp(-h) + \exp(-h_1)}{2} \quad (10c)$$

$$B_i^{**} = \frac{\exp(-h) - \exp(-h_1)}{2} B_i \quad (10d)$$

are the abscissae and weights of the Gauss Points *NGP*, where x_i and B_i represent the standard coordinates and weights of a Gauss integration performed with extremes of integration between -1 and $+1$. Using 3 Gauss Points, the maximum relative error in the integral computation is equal to 2%. This error rapidly decreases to $8 \times 10^{-5} \%$ when 10 integration points are used.

2.2 Case II: surface treatment of an initially homogeneous rough surface

Let us consider each asperity as non-uniform, as sketched in Fig. 5(a). The composite Young's modulus $E^*(\hat{z})$ is now dependent on the \hat{z} coordinate (whose origin is set in the centre of the spherical asperity) and is assumed to vary from E^* at $\hat{z} = 0$ up to γE^* at $\hat{z} = \rho$ according to a linear profile

$$E^*(\hat{z}) = E^* + \frac{(\gamma-1)E^*\hat{z}}{\rho} \quad (11)$$

Similarly to the previous case, for $\gamma > 1$ we have a *positive grading* and the elastic modulus is an increasing function of y . On the other hand, for $\gamma < 1$, we have a *negative grading*. The case with $\gamma = 1$ marks the transition between these two types of grading and corresponds to a homogeneous asperity with $E^*(\hat{z}) = E^*$.

[Figure 5 about here]

The constitutive law of a simple homogeneous asperity relating the applied force, p_{HOM} , to the normal compliance, w , is described by the Hertzian law:

$$p_{\text{HOM}} = \frac{4}{3}\rho^{1/2}w^{3/2}E^* \quad (12)$$

On the other hand, in case of a heterogeneous asperity, dimensional analysis arguments show that the function $p(w)$ will have the following power-law form (Giannakopoulos and Suresh, 1997a,b) if the grading is also of power-law form:

$$p_{\text{FGM}} = \frac{4}{3}\rho^\kappa w^{2-\kappa} E^* f \quad (13)$$

where the parameter f and the exponent κ are both dependent on the prescribed grading. More general functions are to be expected in other cases. However, the form (13) greatly simplifies the GW analysis, which permits us to approximate the numerical results obtained using the finite elements. Therefore, the parameters f and κ will be used as best-fitting parameters. By comparing Eq. (13) and Eq. (12), it is easy to see that the homogeneous Hertzian case, p_{HOM} , is simply recovered as a special case of Eq. (13) when $f=1$ and $\kappa=1/2$. It is also interesting to evaluate the ratio between p_{FGM} and p_{HOM}

$$\frac{p_{\text{FGM}}}{p_{\text{HOM}}} = \left(\frac{w}{\rho}\right)^{2-\kappa-\frac{3}{2}} f = \left(\frac{w}{\rho}\right)^{\frac{1}{2}-\kappa} f \quad (14)$$

To determine f and κ , let us consider an axisymmetric finite element model of the asperity in contact with a rigid body shown in Fig. 5(a). For numerical purposes, the linear grading is approximated by considering a discrete variation of the elastic modulus in ten layers, each one having a depth equal to $\Delta\hat{z} = \rho/10$. The nonlinear contact

problem is solved by enforcing the unilateral contact condition according to the penalty method (see (Zavarise and Schrefler, 1995; Wriggers, 2002; Paggi et al., 2006) for more details). During the simulation, vertical displacements are prescribed to the nodes pertaining to the horizontal diameter. The corresponding force p_{FGM} acting on the sphere is computed a posteriori as the sum of the reaction forces in the same nodes. A deformed configuration with a superimposed contour plot of the displacements is depicted in Fig. 5(b). The ratio between the loads in Eq. (14) is then computed and plotted vs. w/ρ in Fig. 6 for different values of γ (negative and positive gradings). For negative grading ($\gamma < 1$), the FGM sphere is more compliant than the homogeneous one for a given imposed deformation and therefore the ratio (14) is less than unity. For positive grading ($\gamma > 1$), the situation is the opposite and the ratio is always higher than unity.

[Figure 6 about here]

From the bilogarithmic diagram in Fig. 6 we compute the exponent $1/2 - \kappa$ for each value of γ , as the slope of the best-fitting straight lines. Similarly, the parameter f is found from the vertical coordinates of the points of such best-fitting curves in correspondence of $w/\rho = 1$. These results are reported in Fig. 7 and we note that the exponent $1/2 - \kappa$ varies approximately between -0.1 and 0.3 . This variation is more pronounced in case of negative grading. Similarly, the parameter f varies between 0.5 and 3.2 , with a pronounced variation in case of positive grading.

[Figure 7 about here]

These results can be directly included in the generalized Greenwood and Williamson contact theory by noting that the dimensionless normal compliance of a generic asperity, w , is represented by the difference $s - h$ in Eq. (4). Hence, according to the new constitutive law in Eq. (13), Eq. (4) changes as follows

$$P^{\text{II}} = \frac{4}{3} A_n \eta E^* \rho^\kappa \sigma^{2-\kappa} f \frac{1}{\sqrt{2\pi}} \int_h^\infty (s-h)^{2-\kappa} \exp(-0.5s^2) ds \quad (15)$$

To solve Eq. (15) numerically, we consider again the change of variable $t = \exp(-s)$. In this way, the integration limits become finite and we get

$$P^{II} = \frac{4}{3} A_n \eta E^* \rho^\kappa \sigma^{2-\kappa} f \frac{1}{\sqrt{2\pi}} \int_0^{\exp(-h)} (-\ln t - h)^{2-\kappa} \exp\left(-\frac{\ln^2 t}{2}\right) \frac{1}{t} dt \quad (16)$$

Now a suitable application of the Gauss-Legendre quadrature method gives:

$$P^{II} = \frac{4}{3} A_n \eta E^* \rho^\kappa \sigma^{2-\kappa} f \frac{1}{\sqrt{2\pi}} \sum_{i=1}^{NGP} B_i^* (-\ln x_i^* - h)^{2-\kappa} \exp\left[-(\ln x_i^*)^2 / 2\right] \frac{1}{x_i^*} \quad (17)$$

and the summation is extended to all the Gauss Points *NGP* with abscissae $x_i^* = \exp(-h)(1 + x_i)/2$ and weights $B_i^* = \exp(-h)B_i/2$, where x_i and B_i represent the standard coordinates and weights of a Gauss integration performed with integration extremes -1 and $+1$. Also in this case, 10 Gauss Points are sufficient to achieve a relative error in the integral computation less than 8×10^{-5} %.

3. The effect of graded elasticity on the contact behaviour of rough surfaces

3.1 Effects on the slope of the real contact area-load relationship

The relationship between real contact area vs. load is a fundamental quantity in tribological applications and several researchers have argued even recently about its linearity, see, e.g., (Archard, 1957; Persson, 2000; Hyun et al., 2004; Pei et al., 2005; Hyun and Robbins, 2007; Carbone and Bottiglione, 2008; Paggi and Ciavarella, 2010). To estimate its deviation from linearity, the secant ratio between real contact area and load, A/P , is often used instead of computing the tangent to the curve at each load level. For a homogeneous rough surface we have from Eqs. (1) and (2)

$$\left(\frac{A}{P}\right)_{\text{HOM}} = \frac{3\pi\rho^{1/2}}{4\sigma^{1/2}E^*} \frac{F_1(h)}{F_{3/2}(h)} \quad (18)$$

In Case I, where the grading is due to homogeneous asperities with elastic modulus dependent on the height above the surface datum, we have

$$\left(\frac{A}{P}\right)_{\text{FGS}}^{\text{I}} = \begin{cases} \frac{3\pi\rho^{1/2}}{4\sigma^{1/2}E^*} \frac{F_1(h)}{F_{3/2}(h)}, & \text{for } h_1 \leq h < \infty \\ \frac{3\pi\rho^{1/2}}{4\sigma^{1/2}E^*} F_1(h) \\ \frac{F_{3/2}(h) + \frac{\alpha}{\sqrt{2\pi}} \int_h^{h_1} (s-h)^{3/2} \exp\left(-\frac{s^2}{2}\right) (s-h_1) ds}{F_{3/2}(h) + \frac{\alpha}{\sqrt{2\pi}} \int_h^{h_1} (s-h)^{3/2} \exp\left(-\frac{s^2}{2}\right) (s-h_1) ds}, & \text{for } h \leq h_1 \end{cases} \quad (19)$$

To assess the effect of graded elasticity, it is convenient to evaluate the ratio between the graded prediction (19) and the homogeneous one in Eq. (18), in order to obtain a dimensionless number:

$$R^{\text{I}} = \frac{\left(\frac{A}{P}\right)_{\text{FGS}}^{\text{I}}}{\left(\frac{A}{P}\right)_{\text{HOM}}} = \begin{cases} 1, & \text{for } h_1 \leq h < \infty \\ \frac{F_{3/2}(h)}{F_{3/2}(h) + \frac{\alpha}{\sqrt{2\pi}} \int_h^{h_1} (s-h)^{3/2} \exp\left(-\frac{s^2}{2}\right) (s-h_1) ds}, & \text{for } h \leq h_1 \end{cases} \quad (20)$$

which depends on the mean plane separation h , on the grading cut-off height h_1 and on the grading parameter α . The ratio R^{I} is shown in Fig. 8(a) for a mean plane separations $h=1.0$ and four different values of $h_1=1.0, 2.0, 3.0, 4.0$. For $h=h_1$ all the asperities in contact have the same elastic modulus E^* and therefore $R^{\text{I}}=1$. For $h < h_1$, the asperities in the range $h_1 < s < \infty$ have $E^*(s)=E^*$, whereas in the range $h < s < h_1$ their elastic modulus can be either higher than E^* for a negative grading ($\alpha < 0$), or lower than E^* for a positive grading ($\alpha > 0$). The maximum value of α in order to have $E^* > 0$ for all the asperities with $s > 0$ is $\alpha_{\text{max}}=1/h_1$. For $\alpha > 0$, the asperities are more compliant than those of the reference homogeneous surface. Hence, the load applied to the FGS is lower than that applied to the homogeneous surface for a given mean plane separation or, equivalently, for a given real contact area. Consequently, the ratio R^{I} is higher than unity. The opposite situation is observed when $\alpha < 0$. In both cases, the higher h_1 , the higher is the effect on the ratio R^{I} . The limit case represented by $\alpha = 0$ corresponds to the behaviour of a homogeneous surface, leading to $R^{\text{I}} = 1$.

The effect of the mean plane separation on the ratio R^{I} is also relevant, as shown in

Fig. 8(b) by selecting $h_1 = 4.0$ and considering four different mean plane separations $h = 1.0, 2.0, 3.0, 4.0$. The lower h , the higher the effect on R^I .

[Figure 8 about here]

Regarding Case II, where the grading is the result of locally nonhomogeneous asperities, we have

$$\left(\frac{A}{P}\right)_{\text{FGS}}^{\text{II}} = \frac{3\pi\rho^{1-\kappa}\sigma^{\kappa-1}}{4E^*} \frac{F_1(h)}{\frac{f}{\sqrt{2\pi}} \int_h^\infty (s-h)^{2-\kappa} \exp(-0.5s^2) ds} \quad (21)$$

The ratio between the graded prediction (21) and the homogeneous one in Eq. (18) gives:

$$R^{\text{II}} = \frac{\left(\frac{A}{P}\right)_{\text{FGS}}^{\text{II}}}{\left(\frac{A}{P}\right)_{\text{HOM}}} = \left(\frac{\rho}{\sigma}\right)^{1/2-\kappa} \frac{F_{3/2}(h)}{\frac{f}{\sqrt{2\pi}} \int_h^\infty (s-h)^{2-\kappa} \exp(-0.5s^2) ds} \quad (22)$$

The ratio R^{II} depends on the mean plane separation h , on the grading parameter γ through the exponent $\kappa(\gamma)$ and the coefficient $f(\gamma)$, as well as on the ratio ρ/σ . This latter quantity is a random variable that depends on the spectral moments m_0 and m_4 of the rough surface (Zavarise et al., 2007). For fractal surfaces simulated using the random midpoint displacement algorithm (Paggi and Ciavarella, 2010), this ratio lies in the range between 1×10^2 and 1×10^5 , as shown in Fig. 9(a) for fractal surfaces with a lower cut-off length equal to $1/2^n$ ($n=8$) and different fractal dimensions ($D=2.3, 2.5, 2.7, 2.9$). The variation of the lower cut-off length of the system gives also to a similar variability of ρ/σ , as shown in Fig. 9(b) for $D=2.3$ and different lower cut-off lengths $1/2^n$ ($n=6, 7, 8, 9$).

[Figure 9 about here]

The ratio R^{II} is plotted in Fig. 10(a) for different values of ρ/σ and for $h = 1.0$. It is a decreasing function of the grading parameter γ . For this type of grading, the

reference value of the elastic modulus for the homogeneous surface is the value of the elastic modulus evaluated at the centre of the asperity. Therefore, in case of negative grading, the asperities are more compliant than those of a homogeneous surface and the load applied to the FGS is lower than that applied to the homogeneous surface for a given mean plane separation. Consequently, R^{II} is higher than unity. In case of positive grading, the trend is reversed and, for a given real contact area, the load required to deform the FGS is higher than that applied to the homogeneous surface. The ratio R^{II} is significantly affected by the parameter ρ/σ and it is an increasing function of it, implying that the effect of grading is more pronounced in smooth surfaces characterized by low fractal dimensions. On the other hand, the dependency of R^{II} on the mean plane separation is negligible, as shown in Fig. 10(b) for $\rho/\sigma = 1 \times 10^2$ and four different values of h .

[Figure 10 about here]

A comparison between the two types of grading can be performed by examining Figs. 8(a) and 10(a). In general, Case II gives the maximum deviation from unity, implying that the surface treatment of an initially homogeneous rough surface is more effective than a non-uniform erosion of a plane heterogeneous solid. However, similar values of R^{I} and R^{II} can be obtained when $h_1 \square h$, i.e., when the grading in Case I has the highest effect, and when ρ/σ is between 1×10^2 and 1×10^3 , i.e., for surfaces with high fractal dimensions or high resolutions.

3. Preliminary extensions to the plastic field

Related implications of the elastic grading on the plasticity index are also expected. This index can be regarded as the ratio between the mean pressure under elastic deformations and the mean pressure under plastic deformation, which can be assumed equal to the Vickers hardness $H = (P/A)^{\text{plastic}}$ of the softer material (Rabinowicz, 1995). When ψ is less than unity, the asperities deform elastically, otherwise plastic deformations are expected to occur. In formulae:

$$\psi = H / \left(\frac{A}{P} \right)^{\text{elastic}} . \quad (23)$$

If the hardness of the graded surface is the same as that of the homogeneous one, with also the same dependencies on the indentation depth, then the plasticity index of a FGS is equal to the plasticity index of the homogeneous surface divided by the ratio R^i ($i=I$ or II), depending on the considered type of grading:

$$\psi_{\text{FGS}}^i = \frac{\psi_{\text{HOM}}}{R^i} \quad (24)$$

Hence, the inverse of the ratios R^i governs the value of the plasticity index of a FGS with respect to a homogenous surface. The inverse of these ratios, which can be easily deduced from the previous plots in Fig. 8 and 10, ranges from 0.05 to 2, significantly modifying the plasticity index of a rough surface and its mode of deformation.

If the hardness of the FGS is different from that of the homogeneous surface, then the hardness profiles obtained from indentation tests have also to be considered in the analysis. This is however out of the scopes of the present work and can be the subject of future investigations.

4. Discussion and conclusion

In this paper, the Greenwood and Williamson contact theory for microscopically rough surfaces has been generalized in order to model two different types of FGS originating by: (I) a non-uniform erosion of a layered (or functionally graded) solid, or (II) a surface treatment or a chemical degradation of an initially homogeneous rough surface. In Case I we have considered a linear grading on the Young's modulus, introducing an additional dimensionless length scale h_1 which defines the position of the grading cut-off. As a result, the Young's modulus which depends on the asperity height has been included in the integration for the computation of the applied load. In Case II, each asperity has been considered as locally heterogeneous, which leads to a modification of the Hertzian law for the asperity behaviour. This modification has been investigated by performing finite element simulations and then approximating the results using a power-law equation. In this case, the dimensionless number given by the ratio between the asperity radius of curvature and the r.m.s. of asperity heights, ρ/σ , turns out to be

particularly important, since it depends on the resolution and on the fractal dimension of the rough surface.

In both the examined cases, we have demonstrated that graded elasticity has an effect on the slope of the real contact area-load relationship. In Case I, the effect of grading is maximized (maximum deviation from the response of the homogeneous rough surface) when $h_1 \ll h$. In Case II, the effect of grading is in general more pronounced than for Case I. The highest effect is achieved for high values of the ratio ρ/σ , which is a situation that can be found in fractal rough surfaces with low fractal dimensions. For certain mechanical and geometrical configurations, Case I and Case II are equivalent to each other.

Preliminary comments on the related implications of grading on the plasticity index of rough surfaces have finally been proposed. Further investigation in this direction is however necessary, considering indentation-dependent hardness profiles obtained from experiments.

Acknowledgements

MP would like to thank the Alexander von Humboldt Foundation for supporting his research fellowship at the Institut für Kontinuumsmechanik, Leibniz Universität Hannover (Hannover, Germany). The financial support of MIUR to the PRIN2008 project “Advanced applications of fracture mechanics for the study of integrity and durability of materials and structures” is also gratefully acknowledged.

References

- Archard JF (1957) Elastic deformation and the laws of friction, *Proc. Roy. Soc. Lond., Ser. A*, **243**, 190-205.
- Bush AW, Gibson RD, Thomas TR (1975) The elastic contact of a rough surface, *Wear*, **35**, 87-111.
- Carbone G, Bottiglione F (2008) Asperity contact theories: Do they predict linearity between contact area and load?, *Journal of the Mechanics and Physics of Solids*, **56**, 2555-2572.
- Ciavarella M, Greenwood JA, Paggi M (2008) Inclusion of "interaction" in the Greenwood & Williamson contact theory, *Wear*, **265**, 729-734.

- Gao H, Ji B, Buehler MJ, Yao H (2004) Flaw tolerant nanostructures of biological materials, *Mechanics of the 21st Century, Proc. of the 21st International Congress of Theoretical and Applied Mechanics*, Warsaw, Poland.
- Giannakopoulos AE, Suresh S (1997a) Indentation of solids with gradients in elastic properties: Part I. Point force, *International Journal of Solids and Structures*, **34**, 2357-2392.
- Giannakopoulos AE, Suresh S (1997b) Indentation of solids with gradients in elastic properties: Part II. Axisymmetric indenters, *International Journal of Solids and Structures*, **34**, 2393-2428.
- Greenwood JA (2006) A simplified elliptic model of rough surface contact, *Wear*, **261**, 191-200.
- Greenwood JA, Williamson JBP (1966) The contact of nominally flat surfaces, *Proc. R. Soc. London A*, **295**, 300-319.
- Hegazy AAH (1985) Thermal joint conductance of conforming rough surfaces: effect of surface micro-hardness variation, Ph.D. Thesis, University of Waterloo.
- Hyun S, Pei L, Molinari J-F, Robbins MO (2004) Finite-element analysis of contact between elastic self-affine surfaces, *Physical Review E*, **70**, 026117.
- Hyun S, Robbins MO (2007) Elastic contact between rough surfaces: effect of roughness at large and small wavelengths, *Tribology International*, **40**, 1413-1422.
- Lee D., Barber JR, Thouless MD (2009) Indentation of an elastic half space with material properties varying with depth, *International Journal of Engineering Science*, **47**, 1274-1283.
- Liu T-J, Wang Y-S, Zhang C (2008) Axisymmetric frictionless contact of functionally graded materials, *Arch. Appl. Mech.*, **78**, 267-282.
- McCool J (1990) Elastic contact of coated rough surfaces, In *Proc. Leeds-Lyon Symposium on Mechanics of Coatings*, **16**, 157-165.
- McCool J (1992) Nongaussian effects in microcontact, *Int. J. Mach. Tools Manufact.*, **32**, 115-123.
- McCool J (2000) Extending the capability of the Greenwood Williamson microcontact model, *ASME J. Trib.*, **122**, 496-502.
- Mikic BB (1974) Thermal contact conductance: theoretical considerations, *Int. J. Heat Mass Trans.*, **205**, 416-417.
- Morandi Cecchi M, Pirozzi E, Zavarise G (1995) Numerical evaluation of special integrals with application to contact problems, *Proc. Advanced Mathematical Tools in Metrology II*, (P. Ciarlini, M.G. Cox, F. Pavese, D. Richter Eds.), 182-193, Oxford, UK.
- Nayak PR (1971) Random process model of rough surfaces, *ASME J. Lubr. Technol.*, **93**, 398-407.
- Paggi M, Carpinteri A, Zavarise G (2006) A unified interface constitutive law for the study of fracture and contact problems in heterogeneous materials, In: Wriggers P, Nackenhorst U (eds) *Analysis and Simulation of Contact Problems*, Lecture Notes in Applied and Computational Mechanics, Springer-Verlag, Berlin, **27**, 297-304.

- Paggi M., Ciavarella M. (2010) The coefficient of proportionality κ between real contact area and load, with new asperity models, *Wear*, **268**, 1020-1029.
- Pei L, Hyun S, Molinari J-F, Robbins MO (2005) Finite element modelling of elasto-plastic contact between rough surfaces, *Journal of the Mechanics and Physics of Solids*, **53**, 2385-2409.
- Persson NJ (2000) *Sliding Friction: Physical Principles and Applications*, Springer, Berlin, Germany.
- Rabinowicz E (1995) *Friction and Wear of Materials*, Wiley, New York.
- Sherge M, Gorb S (2001) *Biological Micro- and Nano-Tribology – Nature's Solutions*, Springer, Berlin.
- Sridhar MR, Yovanovich MM (1994) Review of elastic and plastic contact conductance models: comparison with experiments, *J. Thermophys. Heat Trans.*, **8**, 633-640.
- Yovanovich MM (2005) Four decades of research on thermal contact, gap, and joint resistance in microelectronics, *IEEE Transactions on Components and Packaging Technologies*, **28**, 182-206.
- Wriggers P (2002) *Computational Contact Mechanics*. John Wiley & Sons, Ltd., The Atrium, Southern Gate, Chichester, West Sussex, PO19 8SQ, England.
- Zavarise G, Borri-Brunetto M, Paggi M (2004) On the reliability of microscopical contact models, *Wear*, **257**, 229-245.
- Zavarise G, Borri-Brunetto M, Paggi M (2007) On the resolution dependence of micromechanical contact models, *Wear*, **262**, 42-54.
- Zavarise G, Wriggers P, Stein E, Schrefler B (1992) A numerical model for thermomechanical contact based on microscopic interface laws, *Mech. Res. Commun.*, **19**:173-182.
- Zavarise G, Schrefler BA (1995) Numerical analysis of microscopically elastic contact problems, in: J.J. Moreau, M. Raous, M. Jean (Eds.), *Contact Mechanics*, Plenum Press, New York, 305-312.

List of Figures

Figure 1: Example of elastic grading in metal systems as a result of surface treatment and chemical degradation (adapted from (Rabinowicz, 1995)).

Figure 2: Cross section of an adhesion pad of a cicada (adapted from (Sherge and Gorb, 2001)).

Figure 3: Sketch of a FGS whose asperities have an elastic modulus dependent on their height.

Figure 4: Linear grading of the elastic modulus for Case I.

Figure 5: Contact between a functionally graded asperity and a rigid plane.

Figure 6: Normal force ratio in Eq. (14) vs. w/ρ for a functionally graded asperity with linear grading.

Figure 7: Parameters κ and f in Eq. (14) vs. γ for a functionally graded asperity with linear grading.

Figure 8: Ratio R^I vs. the grading parameter α . The effect of h_1 (a) and the effect of h (b).

Figure 9: Ratio ρ/σ for fractal rough surfaces with different fractal dimensions D and resolutions $1/2^n$.

Figure 10: Ratio R^{II} vs. the grading parameter γ . The effect of ρ/σ (a) and the effect of h (b).

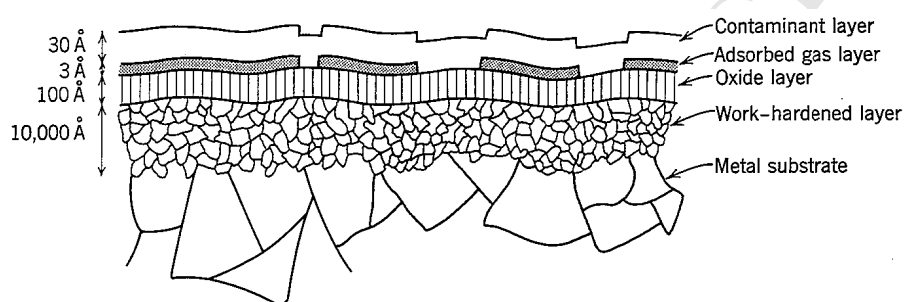


Figure 1

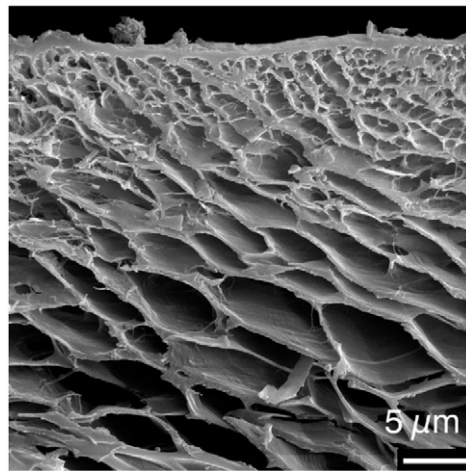
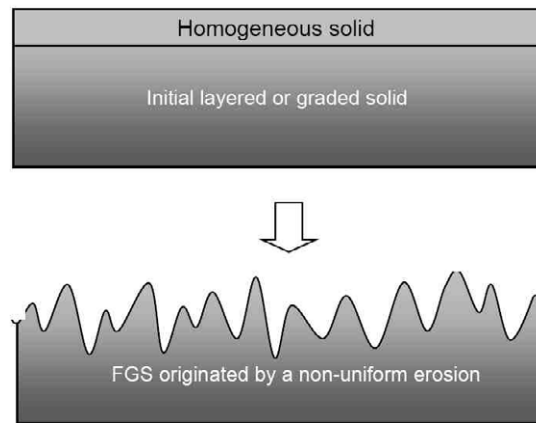
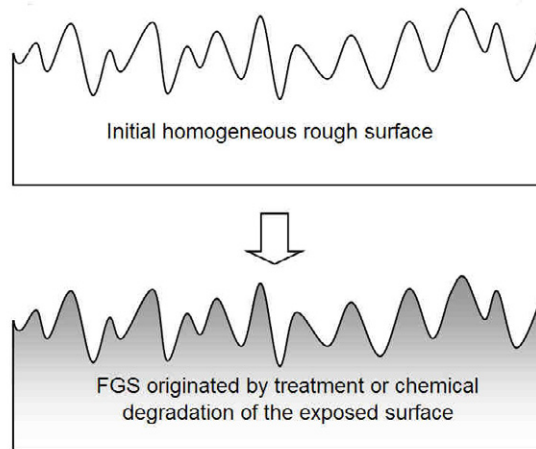


Figure 2



(a) Case I



(b) Case II

Figure 3

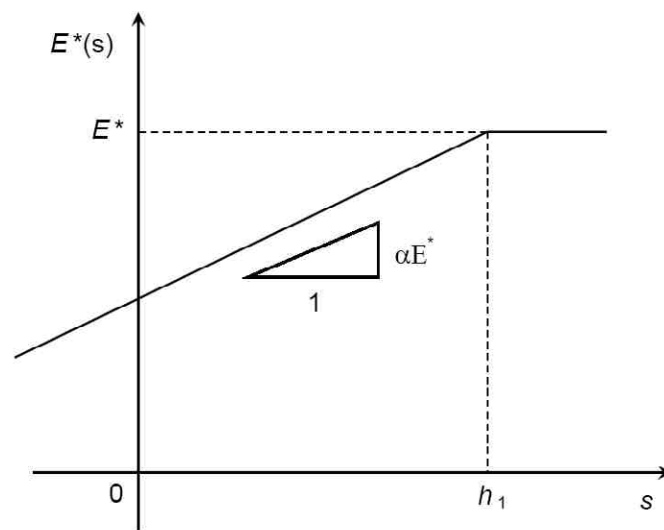


Figure 4

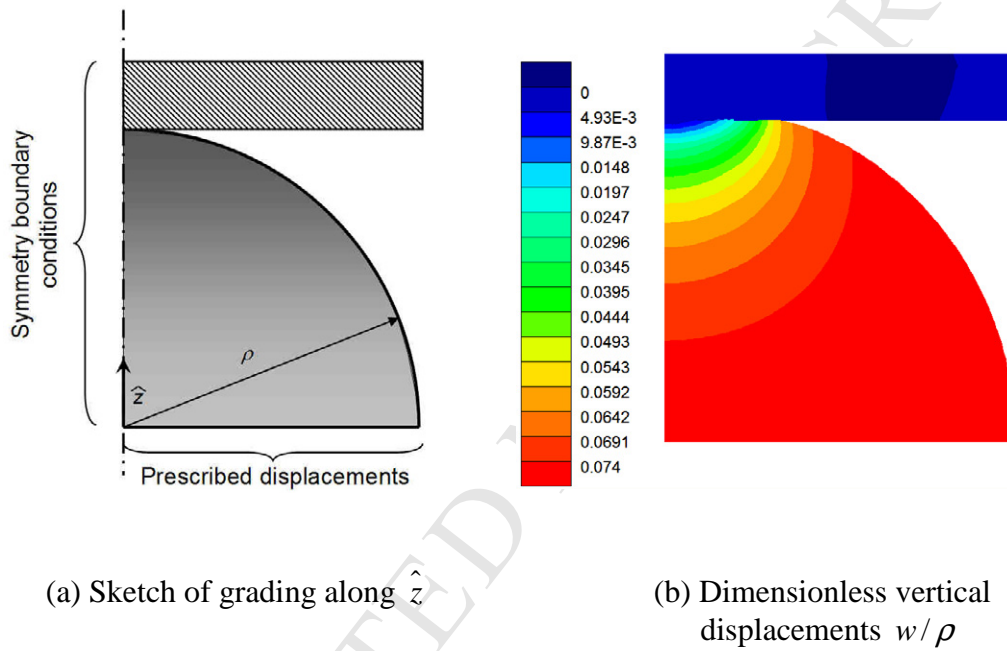


Figure 5

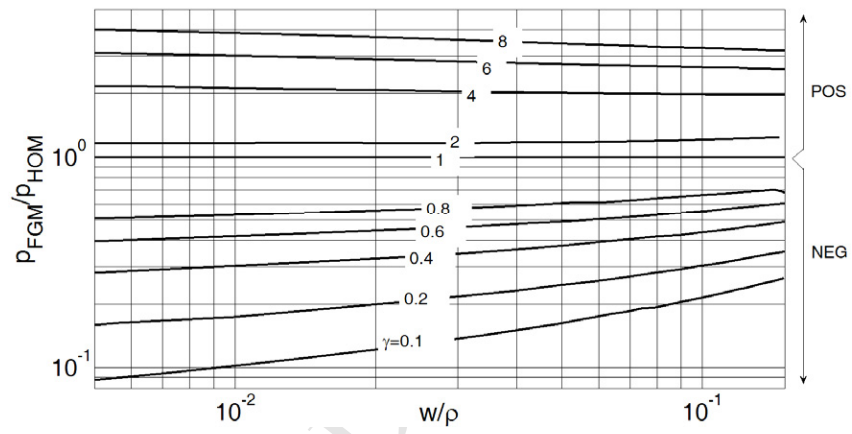


Figure 6

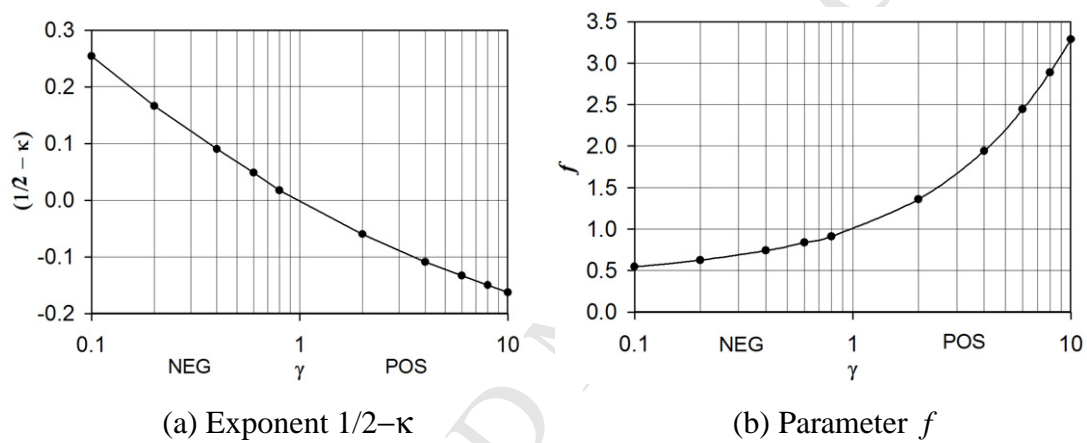


Figure 7

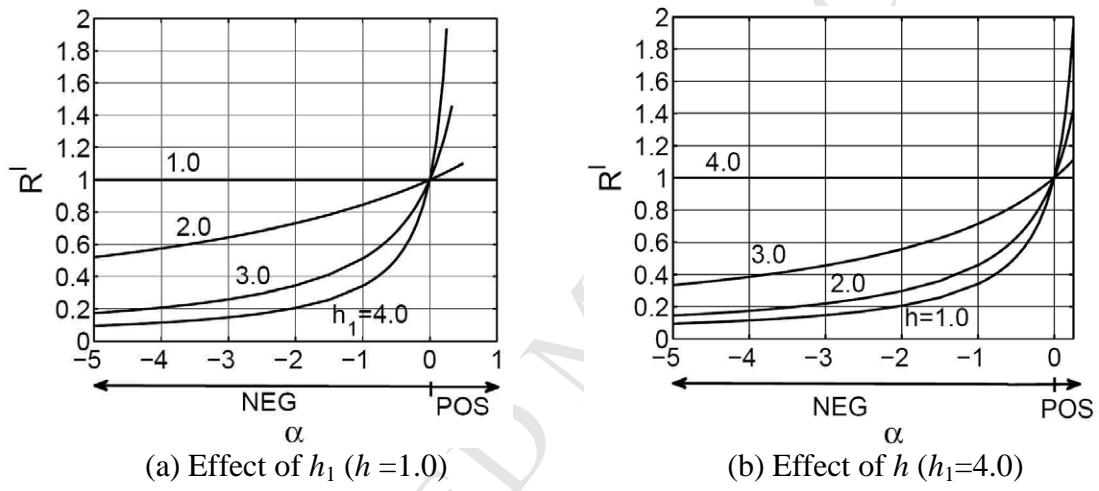


Figure 8

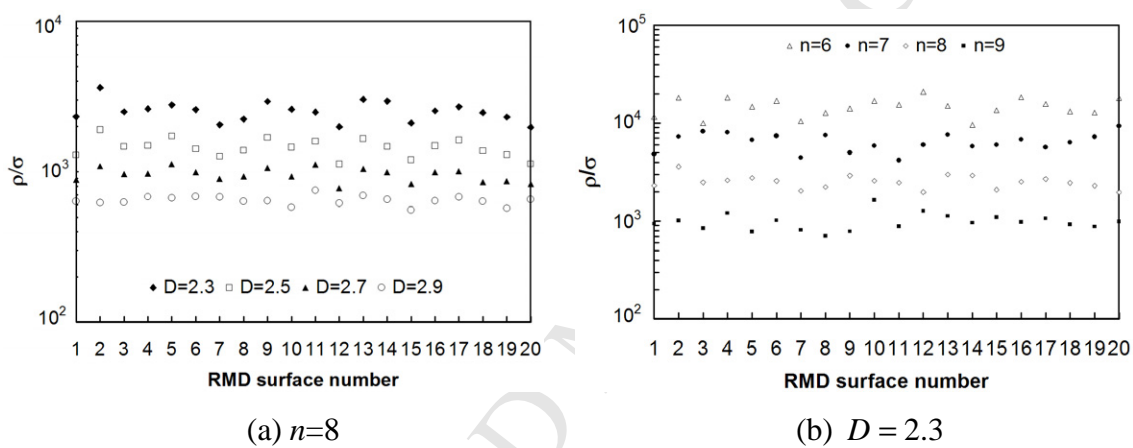


Figure 9

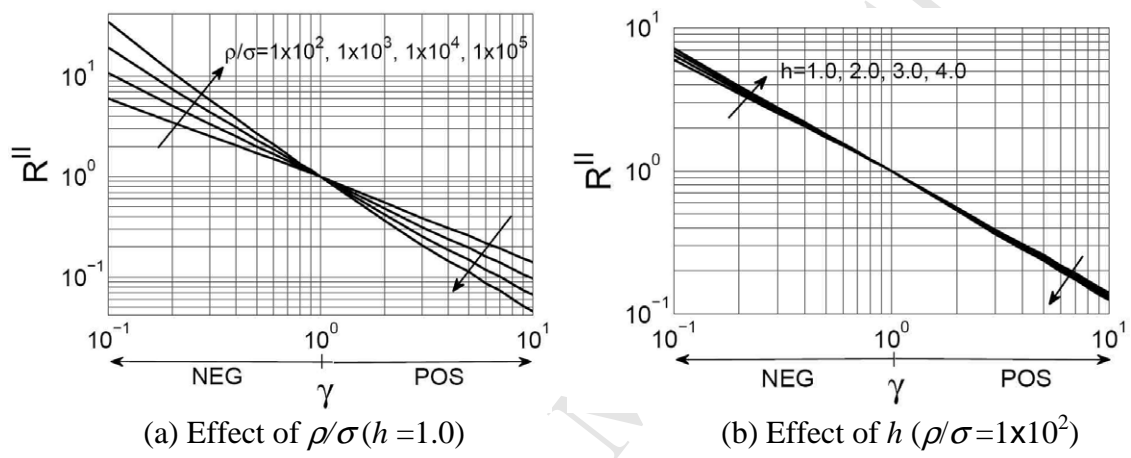


Figure 10